Search for supersymmetry in the photon(s) plus missing energy channels at $\sqrt{s} = 161$ GeV and 172 GeV

The ALEPH Collaboration

Abstract

Searches for supersymmetric particles in channels with one or more photons and missing energy have been performed with data collected by the ALEPH detector at LEP. The data consist of 11.1 pb^{-1} at 161 GeV, 1.1 pb^{-1} at 170 GeV and 9.5 pb^{-1} at 172 GeV. The data are in good agreement with predictions based on the Standard Model, and are used to set upper limits on the cross sections for anomalous photon production. These limits are compared to two different SUSY models and used to set mass limits on the neutralino.

Contribution to lepton-photon conference, Hamburg, 1997

1 Introduction

Events with photons, missing energy and nothing else detected can give insight into possible new physics. Such events have been studied in e^+e^- annihilation at center-of-mass energies around 133 GeV [1] and 161 GeV [2]. The Standard Model(SM) predicts events with photons and missing energy in the form of radiative returns to the Z ($e^+e^- \rightarrow \gamma$ Z) with Z$\rightarrow \nu\bar{\nu}$ and t-channel W exchange where the electron, positron, and/or the virtual W bremsstrahlung one or more photons. Both these processes give $e^+e^- \rightarrow \nu\bar{\nu}\gamma(\gamma)$ events. The $e^+e^- \rightarrow \nu\bar{\nu}\gamma(\gamma)$ process is well understood in the framework of the SM, and any significant deviation from the SM predictions would signal new physics. Supersymmetry can give rise to events where one or more photons are accompanied by weakly interacting supersymmetric particles, seen only as missing transverse energy.

Recently, the CDF collaboration observed an unusual event with two high energy electrons, two high energy photons, and a large amount of missing transverse energy [3]. There is no obvious SM explanation for this event, however it fits nicely into several supersymmetric models. In the Minimal Supersymmetric Standard Model (MSSM) the second lightest neutralino χ_2 can radiatively decay into the lightest neutralino χ_1 and a photon [4]. In this framework the CDF event could then be explained by the Drell-Yan process $q\bar{q} \rightarrow \tilde{e}\tilde{e} \rightarrow ee\chi_2\chi_2 \rightarrow ee\chi_1\chi_1\gamma\gamma$ where the two χ_1's escape detection resulting in missing transverse energy. If this is the explanation for the CDF event, the best possibility for discovery at LEP is $e^+e^- \rightarrow \chi_2\chi_2 \rightarrow \chi_1\chi_1\gamma\gamma$, seen in the detector as two acoplanar photons and missing transverse energy. However, the decay $\chi_2 \rightarrow \chi_1\gamma$ has a significant Branching Ratio in only a small region of parameter space and to be compatible with the kinematics of the CDF event the GUT relation must be broken [5].

Alternatively there are SUSY models where the gravitino is the lightest supersymmetric particle (LSP) and the χ_1 is the next to lightest supersymmetric particle (NLSP). Both No-Scale Super-Gravity [6] and Gauge-Mediated SUSY Breaking [7, 8, 9, 10] theories predict an essentially massless gravitino ($M_{\tilde{G}} < 1$ MeV) and a 100% Branching Ratio for $\chi_1 \rightarrow \tilde{G}\gamma$. The CDF event can be explained (predicted some theorists might say) naturally by these theories. In gravitino LSP models, the CDF event could be explained by $q\bar{q} \rightarrow \tilde{e}\tilde{e} \rightarrow ee\chi_1\chi_1 \rightarrow ee\tilde{G}\tilde{G}\gamma\gamma$. The best channel for discovery at LEP is $e^+e^- \rightarrow \chi_1\chi_1 \rightarrow \tilde{G}\tilde{G}\gamma\gamma$, seen in the detector as two acoplanar photons and missing transverse energy [1]. However, if the gravitino mass is light enough ($M_{\tilde{G}} < 10^{-4}$ eV), the first sign of SUSY could be seen in the form of a single photon and nothing else in the detector [11, 12]. The production process in this scenario would be $e^+e^- \rightarrow \chi_1\tilde{G} \rightarrow \tilde{G}\tilde{G}\gamma$.

The above two models have far fewer parameters than the MSSM and are, therefore, much more predictive. The LNZ No-Scale Super-Gravity model is a one parameter model, thus a discovery of the χ_1 and a measurement of its mass would determine the mass of all the other super-partners. Gauge-Mediated SUSY Breaking was first proposed by Fayet in 1977 [13], and was pursued experimentally at PETRA, PEP, and TRISTAN [14]. The mass spectrum of the super-partners in this theory (for the minimal model) depends only on a few parameters.

This note presents the results of a search for supersymmetry in the photon plus missing energy channels at the recent LEP high energy running, where 11.1 pb^{-1} of data at $\sqrt{s} = 161$ GeV and 10.6 pb^{-1} of data at $\sqrt{s} = 170/172$ GeV were recorded in the ALEPH detector.

[1] Of course, one can have the process $e^+e^- \rightarrow \tilde{l}\tilde{l} \rightarrow l^+l^-\tilde{G}\tilde{G}$ at LEP, but for most gravitino LSP models the χ_1 is the least massive superpartner, and therefore can be produced at lower center-of-mass energy. In the minimal model of Gauge-Mediated SUSY Breaking this is always true except at very large tanβ. In the LNZ model this is always true.

2 The ALEPH detector and photon identification

The ALEPH detector and its performance is described in detail elsewhere [15, 16]. The analysis presented here depends largely on the performance of the electromagnetic calorimeter (ECAL). The luminosity calorimeters (LCAL and SICAL), together with the hadron calorimeter (HCAL), are used mainly to veto events where photons are accompanied by other energetic particles. The tracking system, composed of a silicon vertex detector, wire drift chamber (ITC), and time projection chamber (TPC), is used to provide efficient ($> 99.9\%$) tracking of charged particles in the angular range $|\cos\theta| < 0.96$.

The ECAL is a lead/wire-plane sampling calorimeter. It consists of 36 modules, twelve in the barrel and twelve in each endcap, which provide coverage in the angular range $|\cos\theta| < 0.98$. Inter-module cracks reduce this solid angle coverage by 2% in the barrel and 6% in the endcaps. However, the ECAL and HCAL cracks are not aligned so there are no holes in ALEPH at large polar angles. The total thickness of the ECAL is 22 radiation lengths at normal incidence. The longitudinal sampling consists of 45 layers of lead, 2 mm thick in the first 13 radiation lengths (33 layers) and 4 mm thick in the remainder (12 layers). Anode wire signals, sampled every 512 ns during their rise time, provide a measurement by the ECAL of the interaction time t_0 of the particles relative to the beam crossing with a resolution better than 15 ns (for showers with energy greater than 1 GeV). Cathode pads associated with each layer of the wire chambers are connected to form projective "towers", each subtending approximately $0.9° \times 0.9°$, which are oriented towards the interaction point. Each tower is read out in three radial segments (each one called a 'storey') in depth of four, nine and nine radiation lengths. The high granularity of the calorimeter provides excellent identification of photons and electrons. The energy calibration of the ECAL is obtained from Bhabha and gamma-gamma events. The energy resolution is measured to be $\Delta E/E = 0.18/\sqrt{E} + 0.009$ (E in GeV) [16].

Photon candidates are identified using an algorithm [16] which performs a topological search for localised energy depositions within clusters (groups of neighboring ECAL towers with significant energy deposition). These localised energy depositions are required to have a transverse and longitudinal profile consistent with that of an electromagnetic shower. In order to optimize the energy reconstruction, photons that are not well contained in the ECAL (near or in a crack) take their energy from the localized energy deposition summed together with all energy deposits in the HCAL within a cone of $|\cos\alpha| > 0.98$. Photons well contained in an ECAL module take their energy solely from the localized energy deposition. Photon candidates may also be identified in the tracking system if they convert producing an electron-positron pair.

The trigger most relevant for photonic events is the neutral energy trigger. For the 1996 running this trigger required 1 GeV total wire energy in a module for the barrel of the ECAL or 2.3 GeV total wire energy in an endcap module of the ECAL. The neutral energy trigger is completely efficient for the analyses to be described.

3 One photon and missing energy

The Standard Model predicts a large cross section for the process $e^+e^- \to \nu\bar{\nu}\gamma(\gamma)$, which constitutes an irreducible background. One can, however, still search for new physics by observing an excess of events over the Standard Model prediction. For this method to work, there are two important criteria. The process $e^+e^- \to \nu\bar{\nu}\gamma(\gamma)$, which will be used for the background subtraction must be understood, and other sources of background which are not so easily predicted must be reduced to a negligible level.

3.1 *Event selection*

Initially, all photons are required to be inside the acceptance cuts of $|\cos\theta| < 0.95$ and $p_\perp > 0.0375 * \sqrt{s}$ (where $p_\perp$ is defined as the measured transverse momentum relative to the beam axis). The remaining selection criteria are tailored to eliminate as much as possible the non-subtractable backgrounds: cosmic ray events, detector noise events (a spark in an ECAL module for example) and events in which initial or final state particles radiate a photon and escape down the beam axis. Cosmic events that traverse the detector are eliminated if there are charged tracks in the TPC or ITC or if there are hits in the outer part of the HCAL. These cuts are not effective against cosmic events that do not leave a clear pattern in the detector nor against detector noise events. In this case the ECAL information can be exploited. The barycenter (center of gravity of the photon shower) is found in each of the three ECAL layers. Taking two points at a time, three possible photon trajectories are calculated and used to estimate the distance of closest approach of the photon to the interaction point. The smallest of the three distances ('impact parameter of the photon') is required to be less than 25 cm. Shown in Figure 1 is the impact parameter of the photon candidate from $\mathrm{e^+e^-} \to \gamma\gamma(\gamma)$ events (both data and Monte Carlo) compared to cosmic ray events. The compactness of the shower in the ECAL is calculated by taking an energy-weighted average of the angular deviation (with respect to the interaction point) from the cluster barycenter to the barycenter of each of the ECAL storeys contributing to the cluster. This compactness is required to be less than 0.85°. Finally, the interaction time is required to be within 40 ns of the beam crossing.

A single photon and missing energy might also be caused by initial state radiation (or final state radiation) when the radiating particle escapes down the beam direction. The measured $p_\perp$ of the photon must be greater than $0.0375 * \sqrt{s}$, consequently these events will most of the time have a particle in the angular acceptance of the detector. These events are eliminated by one (or both) of two cuts. There must be no charged tracks in the event not coming from a conversion. In addition, the event is rejected if the total energy excluding photons in the detector is more than 1 GeV or if there is any energy within 14° of the beam axis. This requirement reduces the efficiency for signal by 10% due to additional brehmsstraglung photons at low angles (7% of the loss) and uncorrelated noise in the detector (3% of the loss). To compensate for vertical cracks in the LCAL at azimuthal angles around 90° and 270°, the $p_\perp$ requirement is tightened to $0.145*\sqrt{s}$ if the missing $p_\perp$ points to within 17° of 90° or 270° in azimuthal angle.

Residual cosmic ray and detector noise background was measured by looking for events slightly out of time with respect to the beam crossing but which passed all other cuts. No such events were found in a displaced time window of 740 ns. Events with a photon in the acceptance and a radiating particle escaping undetected down the beam axis were studied using the BHWIDE [18] and $\mathrm{e^+e^-} \to \gamma\gamma(\gamma)$ [19] Monte Carlo. The equivalent of 60 data sets was generated and passed through the full detector simulation. No events from this sample survived the selection.

3.2 *The One photon sample and measurement of the* $\mathrm{e^+e^-} \to \nu\bar{\nu}\gamma(\gamma)$ *cross section*

The efficiency for $\mathrm{e^+e^-} \to \nu\bar{\nu}\gamma(\gamma)$ is estimated using the KORALZ Monte Carlo [17] passed through the full ALEPH detector simulation program, and is detailed in Table 1. The efficiency of the impact parameter and compactness cuts are checked using an $\mathrm{e^+e^-} \to \gamma\gamma(\gamma)$ sample from $\sqrt{s}$= 161

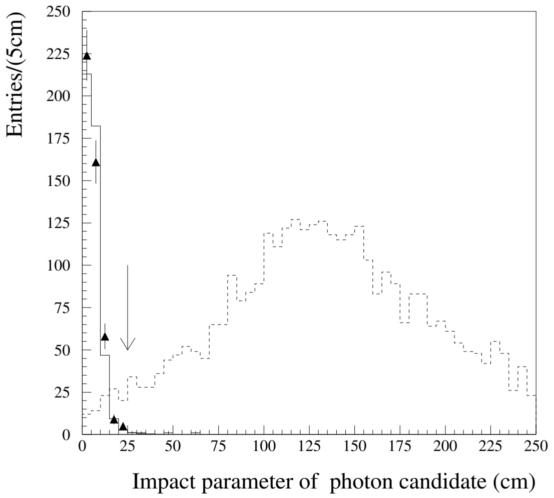

Figure 1: The minimum distance of closest approach to the interaction point of an ECAL object observed in data $e^+e^- \to \gamma\gamma(\gamma)$ events (triangles), in Monte Carlo $e^+e^- \to \gamma\gamma(\gamma)$ events (solid histogram) and in cosmic events (dashed histogram). The only selection criteria applied to the cosmic ray events is that there be no charged tracks in the TPC. The Monte Carlo is absolutely normalized to the data; the cosmic ray events are arbitrarily normalized. The cut at 25 cm is indicated by the arrow.

Cuts	Cumulative signal eff.
Photon reconstruction and no charged tracks in the event that are not associated with a conversion	94%
Number of photons in acceptance = 1	89%
$p_\perp > 0.145 * \sqrt{s}$ when the missing $p_\perp$ points to the LCAL crack	82%
Additional total energy flow < 1 GeV	72%
No energy within 14° of the beam-axis	71%
All other cuts	70%

Table 1: Efficiency for the $e^+e^- \to \nu\bar{\nu}\gamma(\gamma)$ process inside the acceptance cuts at $\sqrt{s} = 161$ GeV.

GeV and 170/172 GeV. The efficiency for photons found in $e^+e^- \to \gamma\gamma(\gamma)$ events in the data and Monte Carlo agree at the 1% level. The efficiency loss due to uncorrelated noise or beam-related background in the detector (approximately 3%) is estimated using events triggered at random beam crossings and is included in the efficiency estimate given in Table 1. Applying the selection criteria to the data, 41 one-photon events are found at $\sqrt{s} = 161$ GeV while 45 one-photon events are expected from Monte Carlo. At $\sqrt{s} = 170/172$ GeV, 36 one-photon events are found while 37 one-photon events are expected.

Inside the acceptance $|\cos\theta| < 0.95$ and $p_\perp > 0.0375 * \sqrt{s}$ the cross sections are

$$\sigma(e^+e^- \to \nu\bar{\nu}\gamma(\gamma)) = 5.3 \pm 0.8 \pm 0.2\,\text{pb} \quad \text{at} \quad \sqrt{s} = 161 \quad \text{GeV}$$

Photon selection	3%
Converted photon selection	0.3%
Energy calibration	0.2%
Background	<1%
Error on efficiency for the impact parameter and compactness of shower cuts	1%
Integrated luminosity	0.7%
Monte Carlo theoretical	<1%
Monte Carlo statistical	0.4%
Total (in quadrature)	4%

Table 2: Systematic errors for the one-photon channel.

$$\sigma(\mathrm{e^+e^-} \to \nu\bar{\nu}\gamma(\gamma)) = 4.7 \pm 0.8 \pm 0.2\,\mathrm{pb} \quad \mathrm{at} \quad \sqrt{\mathrm{s}} = 172 \quad \mathrm{GeV}$$

These results are consistent with the Standard Model predictions of 5.81 $\pm$ 0.03 pb at 161 GeV and 4.85 $\pm$ 0.04 pb at 172 GeV obtained using the Koralz Monte Carlo. The missing mass distribution is shown in Figure 2.

Estimates of the systematic uncertainty in these cross sections are shown in Table 2. The ability of the Monte Carlo to simulate the selection efficiency for energetic photons accurately is checked with a sample of Bhabha events selected using only tracking and muon chamber information. The tracking information was masked from these events and the photon reconstruction redone. The efficiency to reconstruct a photon in these events is found to be consistent between data and Monte Carlo simulation at the 3% level. The uncertainty in the number of simulated pair conversions is estimated to give a 0.3% change in the overall efficiency. To check the energy calibration the energy is shifted by 2% and the efficiency is recalculated. The difference in the efficiency is found to be 0.2 %. The total systematic error is obtained by adding in quadrature the individual contributions.

3.3 *Search for light gravitino in the one photon channel*

In order to find the signal $\mathrm{e^+e^-} \to \chi_1\tilde{\mathrm{G}} \to \tilde{\mathrm{G}}\tilde{\mathrm{G}}\gamma$, a maximum likelihood method is applied to the missing mass spectrum under the hypothesis that there is a mixture of signal and background in the data. Events from the $\mathrm{e^+e^-} \to \nu\bar{\nu}\gamma(\gamma)$ process and the $\mathrm{e^+e^-} \to \chi_1\tilde{\mathrm{G}} \to \tilde{\mathrm{G}}\tilde{\mathrm{G}}\gamma$ process have very different distributions in missing mass, as shown in Figure 2. The binned likelihood that the one-photon missing mass distribution agrees with the composite one-photon missing mass distribution of the Monte Carlo $\mathrm{e^+e^-} \to \nu\bar{\nu}\gamma(\gamma)$ and the signal $\mathrm{e^+e^-} \to \chi_1\tilde{\mathrm{G}} \to \tilde{\mathrm{G}}\tilde{\mathrm{G}}\gamma$ reactions is calculated. Following the method of Ref. [20], the upper limit on the total number of signal events s is calculated by integrating the likelihood as a function of s. The number of signal events is increased until the integration from s=0 to $s = N_s$ of the likelihood is 95% of the total area (the integration from s=0 to $s = \infty$). N_s is then the upper limit on the total number of signal events at the 95% confidence level. This procedure is repeated at each neutralino mass ranging from 40 GeV/c^2 to 171 GeV/c^2 in steps of 1 GeV/c^2.

A toy Monte Carlo with the kinematic cuts applied is used to describe the signal shape of the missing mass distribution at each neutralino mass. Events generated by SUSYGEN [21] and processed through the detector simulation program are used to estimate the efficiency loss due to incident state radiation and photon reconstruction. The efficiency for signal (over the neutralino mass range 40 GeV/c^2 - 172 GeV/c^2) ranges from 70% to 80%, reaching its largest value when M_χ approaches $\sqrt{s}$.

As reported in the previous section, 77 one-photon events are found in the combined data set and 82 are expected from the Monte Carlo. The upper limit on the cross section at 95% confidence level is shown in Figure 3. The upper limit is compared to the predicted cross section from the LNZ theory [12]. For a gravitino mass of 10^{-5} eV/c^2, and selectron mass of 140 GeV/c^2 the mass limit for the neutralino is 100 GeV/c^2. However, the cross section for this process scales as the inverse of the gravitino mass squared, so the limit on the neutralino mass is very sensitive to the assumed gravitino mass.

The systematics are the same as given in the previous section. The change in the number of signal events excluded is less than 1%, following the method of Ref. [22].

4 Two photons and missing energy

As described in the Introduction, there are two SUSY scenarios which can give acoplanar photons: the gravitino LSP and the neutralino LSP scenarios. The signals differ in that the invisible particle is essentially massless in the first scenario and can have substantial mass in the second. This leads to two slightly different search criteria, as described in the subsections below.

The cross section for the SM background process $\nu\bar{\nu}\gamma\gamma$ is reduced by order alpha from the single-photon cross section, so a cut-based analysis is sufficient to search for new physics. Since two photons are required, background from cosmic rays and detector noise is less severe, so the impact parameter and compactness requirements are not imposed. Due to detector acceptance only photons within $|\cos\theta| < 0.95$ are counted. Events with more than two photons are required to have at least $0.4{*}\sqrt{s}$ of missing energy. Missing transverse energy is required by imposing an acoplanarity cut and requiring the additional total energy be less than 1 GeV. When there are three or more photons in the event, the two most energetic photons are used to determine the acoplanarity. The $e^+e^- \to \gamma\gamma(\gamma)$ background is effectively eliminated after this selection criteria. The total $p_\perp$ is required to be greater than 0.0375 of the missing energy reducing background from radiating events down the beam-axis to a negligible level. The selection criteria are shown in Table 3.

After this initial selection, two events are selected at 161 GeV while 2.7 are expected. At 172 GeV, one event is selected and 2.3 are expected.

4.1 *Acoplanar photon search: gravitino LSP scenario*

Additional cuts are placed on the energy of the less energetic photon to reduce substantially the remaining SM background. The energy distribution of the second photon is peaked towards zero for the background, and is flat for the signal in an interval depending on the neutralino mass and $\sqrt{s}$. A cut, set according to the $\bar{\mathrm{N}}95$ optimisation procedure, reduces the background significantly with no cost in efficiency for a high mass neutralino. Using the theoretical cross section for a pure bino neutralino, the optimal cut is 18 GeV for the luminosity taken. With the requirement that the second most energetic photon must be at least 18 GeV, the background is reduced to 0.043 pb^{-1}, while the efficiency remains high at 69% for a neutralino of 65 GeV/c^2 mass produced at 161 GeV. This efficiency was estimated using the SUSYGEN Monte Carlo and setting the parameters so that the χ_1 is pure bino and then adding a new decay (with 100% Branching Ratio) $\chi_1 \to \tilde{G}\gamma$.

Cuts	Cumulative signal eff.	$\nu\bar{\nu}\gamma\gamma(\gamma)$ bkg. X-section (pb)	$\gamma\gamma(\gamma)$ bkg. X-section (pb)
Two-photon selection criteria			
Reconstructed, $\mid \cos\theta \mid < 0.95$, E > 1 GeV, nphot=2.or. (nphot$\geq$3.and.$E_{missing} > 0.4 * \sqrt{s}$)	83%	0.36	11.9
Additional total energy in event < 1 GeV	78%	0.33	10.8
Acoplanarity < 177°	76%	0.32	0.008
Total $p_\perp > 0.0375 * E_{missing}$	76%	0.30	0.002
Efficiency loss due to noise in the detector	73%		
$\tilde{G}$ LSP analysis			
$E_2 \geq 18$ GeV	69%	0.043	0.002
χ_1 LSP analysis			
$M_{missing} \leq 82$ GeV/c^2 OR $M_{missing} \geq 100$ GeV/c^2 OR $E_2 \geq 10$ GeV	71%	0.16	0.002
Two photons inside $\mid\cos\theta\mid < 0.8$	52%	0.063	-

Table 3: Two-photon selection criteria, and the additional cuts required by the two respective analyses. Signal efficiency for the gravitino LSP analysis is quoted for a 65 GeV/c^2 neutralino at $\sqrt{s} = 161$ GeV. For the χ_1 LSP analysis the efficiency numbers are for a 45 GeV/c^2 χ_2 and a 20 GeV/c^2 χ_1. Background numbers are quoted for $\sqrt{s} = 161$ GeV but are similar for 172 GeV.

After this selection criteria no events were found in the data while 0.92 events were expected from background processes. Figure 4 shows the upper limit on the cross section and Figure 5 shows the experimental results compared to two theoretical predictions. The mass limits obtained are:

$$M_{\chi_1} \geq 71\,\mathrm{GeV}/c^2 \quad \text{at} \quad 95\% \quad \text{C.L.}$$

for a pure bino neutralino with $\tau_\chi \leq 3$ ns [2] (applicable to the Gauge-mediated Low Energy SUSY Breaking theory [7, 8], the selectron mass is taken to be 1.5 times the neutralino mass) and

$$M_{\chi_1} \geq 71\,\mathrm{GeV}/c^2 \quad \text{at} \quad 95\% \quad \text{C.L.}$$

(for the LNZ No-Scale Super Gravity one parameter model [6]).
The systematics for this analysis are less than 6%, dominated by photon reconstruction efficiency. The effect of this uncertainty on the cross section upper limits is less then 1% following the method of Ref. [22]. The effect on the mass limit is completely negligible.

In the Gauge-Mediated SUSY Breaking model the neutralino can have a non-negligible lifetime. This lifetime directly depends on the SUSY breaking scale $\sqrt{F}$. The lifetime of the neutralino is given by [7]:

$$c\tau \simeq 130 \left(\frac{100\,\mathrm{GeV/c^2}}{M_\chi}\right)^5 \left(\frac{\sqrt{F}}{100\,\mathrm{TeV}}\right)^4 \mu\mathrm{m}$$

For a neutralino mass of 71 GeV/c^2 with lifetime of 3 ns, the SUSY breaking scale is 600 TeV.

[2]There is no efficiency loss for lifetimes below 3 ns.

Figure 6 shows the 95% C.L. exclusion limit of $\sqrt{F}$ vs. M_χ.

At LEP the production of neutralinos (with neutralino composition pure bino [6, 8]) would proceed via t-channel selectron exchange. Right-handed selectron exchange dominates over left-handed selectron exchange. Thus, the cross section for $e^+e^- \to \chi_1\chi_1$ depends strongly on the right-handed slectron mass and weakly on the left-handed selectron mass. The theoretical cross section for $e^+e^- \to \chi_1\chi_1$ is calculated at each $M_{\tilde{e}_R}$, M_χ mass point for right-handed selectron masses ranging from 70 GeV/c^2 to 200 GeV/c^2 and neutralino masses ranging from 30 GeV/c^2 to 150 GeV/c^2. The neutralino mass limits were also checked for various left-handed selectron masses. The result is found to be robust at the ± 1 GeV/c^2 level for left-handed selectron masses ranging from $M_{\tilde{e}_L} = M_{\tilde{e}_R}$ to $M_{\tilde{e}_L} = 5{*}M_{\tilde{e}_R}$.

The experimental lower limit on the neutralino mass as a function of selectron mass plane is overlayed on the 'CDF region' as shown in Figure 7. The CDF region is the area in the neutralino, selectron mass plane where the properties of the CDF event are compatible with the process $q\bar{q} \to \tilde{e}\tilde{e} \to ee\chi_1\chi_1 \to ee\tilde{G}\tilde{G}\gamma\gamma$. Half of the CDF region is already excluded at 95% C.L. by this analysis.

4.2 *Acoplanar photon search: neutralino LSP scenario*

For the neutralino LSP scenario, a simple energy cut is not optimal since the χ_1 is massive and the photons from the $\chi_2 \to \chi_1\gamma$ decay can have low energy. Here the fact that the $\nu\bar{\nu}\gamma\gamma(\gamma)$ background peaks at large polar angles and has a missing mass at the Z mass is utilized. Events that have missing mass between 82 GeV/c^2 and 100 GeV/c^2, and the energy of the second most energetic photon less than 10 GeV are cut. The $\cos\theta$ cut is optimised by minimizing N95, leading to $|\cos\theta| < 0.8$. We assume a flat $\cos\theta$ distribution for the signal and the Monte Carlo $\cos\theta$ distribution for the $\nu\bar{\nu}\gamma\gamma(\gamma)$ background.

The efficiency is estimated using a large sample of the SUSYGEN Monte Carlo at both 161 and 172 GeV. At $\sqrt{s} = 161$ GeV and $\Delta M \geq 20$ GeV/c^2 (where ΔM is the $\chi_2 - \chi_1$ mass difference) the efficiency varied from 51% to 57% over the χ_2,χ_1 mass plane. For 10 GeV/c^2 $< \Delta M \leq 20$ GeV/c^2 the efficiency varied from 47% to 54% . For 5 GeV/c^2 $\leq \Delta M \leq 10$ GeV/c^2 the efficiency varied from 31% to 47% . The efficiencies at 172 GeV match (within error) those at 161 GeV.

One event is found in the data while 1.3 events are expected from background. The upper limits on the cross sections as a function of χ_1, χ_2 masses are shown to in Figure 8. The branching ratio for $\chi_2 \to \chi_1\gamma$ is assumed to be 100%.

The $\Delta M \geq 20$ GeV/c^2 cross section is interesting in terms of the CDF event, as theoretical predictions for $e^+e^- \to \chi_2\chi_2 \to \chi_1\chi_1\gamma\gamma$ at LEP can be as high as 1 pb. The systematics for this analysis are the same as for the gravitino LSP scenario and the effect of the systematic uncertainty on the cross section upper limits is again less then 1% following the method of Ref. [22].

The χ_1 LSP interpretation of the CDF event (along with the non-observation of other SUSY signatures at Fermilab) suggests a high branching ratio for $\chi_2 \to \chi_1\gamma$. Assuming 100% branching ratio, the lower mass limit of χ_2 as a function of the selectron mass is calculated and compared to the region compatible with the CDF event. In Figure 9a the case $M_{\tilde{e}_L} = M_{\tilde{e}_R}$ is shown. In Figure 9b the case $M_{\tilde{e}_L} = 3{*}M_{\tilde{e}_R}$ is shown. With the assumption that BR($\chi_2 \to \chi_1\gamma$) = 100%, this analysis excludes a significant portion of the region allowed by the CDF event.

5 Conclusion

ALEPH data collected at LEP center of mass energies of 161 GeV and 170/172 GeV show no signs of new physics in the photon(s) plus missing energy channels. The $e^+e^- \to \nu\bar{\nu}\gamma(\gamma)$ cross sections and distributions are in agreement with Standard Model expectations. The experimental 95% C.L. upper limits on the cross sections are derived for the following supersymmetric processes: $e^+e^- \to \chi_1\tilde{G} \to \tilde{G}\tilde{G}\gamma$, $e^+e^- \to \chi_1\chi_1 \to \tilde{G}\tilde{G}\gamma\gamma$ and $e^+e^- \to \chi_2\chi_2 \to \chi_1\chi_1\gamma\gamma$. These cross section limits are actually more general and can be applied to the reactions: $e^+e^- \to \mathrm{XY} \to \gamma\mathrm{YY}$ where Y is massless and $e^+e^- \to \mathrm{XX} \to \gamma\gamma\mathrm{YY}$ where Y is massless or Y has mass. The 95% C.L. limits on the χ_1 mass are set for two different gravitino LSP SUSY scenarios. The excluded region of the SUSY Breaking Scale as a function of neutralino mass is derived. The lower limit on the $\chi_1(\chi_2)$ mass as a function of selectron mass is determined and compared to the region compatible with the CDF event for the gravitino (neutralino) LSP scenario.

References

[1] ALEPH Collab., D. Buskulic et al., Phys. Lett. B384 (1996) 333;
DELPHI Collab., P. Abreu et al., Phys. Lett. B380 (1996) 471;
L3 Collab., M. Acciarri et al., Phys. Lett. B384 (1996) 323;
OPAL Collab., G. Alexander et al., Phys. Lett. B377 (1996) 222.

[2] OPAL Collab., G. Alexander et al., Phys. Lett. B391 (1997) 210.

[3] S. Park, in Proceedings of the 10th Topical Workshop on Proton-Antiproton Collider Physics, Fermilab, 1995, edited by R. Raja and J.Yoh (AIP,New York,1995),p 62.

[4] H. Haber and D. Wyler, Nuclear Physics B323 (1989) 267.

[5] S. Ambrosanio, G. Kane, G. Kribs, S. Martin and S. Mrenna, Phys. Rev. D55 (1997) 1372.

[6] J. Lopez and D. Nanopoulos, Phys. Rev. D55 (1997) 4450.

[7] S. Dimopoulos, M. Dine, S. Raby and S. Thomas, Phys. Rev. Lett. 76 (1996) 3494.

[8] S. Dimopoulos, S. Thomas and J. D. Wells, Nucl. Phys. B488 (1997) 39.

[9] M. Dine, W.Fischler and M. Srednichi, Nucl. Phys. B189 (1981) 575.

[10] M. Dine, A. Nelson and Y. Shirman, Phys. Rev. D51 (1995).

[11] P. Fayet, Phys. Lett. B175 (1986) 471.

[12] J. Lopez and D. Nanopoulos, Phys. Rev. D55 (1997) 5813.

[13] P. Fayet, Phys. Lett. B69 (1977) 489;
P. Fayet, Phys. Lett. B70 (1977) 461.

[14] JADE Collab.,W. Bartel et al., Phys. Lett. B139 (1984) 327;
CELLO Collab., H. J. Behrend et al., Z. Phys. C35 (1987) 181;
VENUS Collab., K. Abe et al., Z. Phys C45 (1989) 175;
ASP Collab., G. Bartha et al., Phys. Rev. D39 (1995) 3207.

[15] ALEPH Collab., D. Decamp et al., Nucl. Instrum. Methods A294 (1990) 121.

[16] ALEPH Collab., D. Buskulic et al., Nucl. Instrum. Methods A360 (1995) 481.

[17] S. Jadach, B.F.L. Ward and Z. Was, Comp. Phys. Commun. 79 (1994) 503.

[18] S. Jadach, W. Placzek and B. F. L. Ward, preprint The University of Tennessee UTHEP-95-1001 (unpublished).

[19] F.A. Berends and R. Kleiss, Nucl. Phys. B186 (1981) 22.

[20] Luca Lista, Nucl. Instrum. Methods A340 (1994) 396;
T. Bayes,*An essay towards solving a problem in the doctrine of chances*, Philosophical Transactions of the Royal Society, 53 (1763) 370, (Reprinted in Biometrika, 45 (1958) 159).

[21] S. Katsanevas and S. Melachroinos, in *Physics at LEP2*, Eds. G. Altarelli, T. Sj östrand, F. Zwirner, CERN Report 96-01, Volume 2 (1996) 328.

[22] R. D. Cousins and V. L. Highland, Nucl. Instrum. Methods A320 (1992) 331.

[23] Gian Giudice, CERN Theory seminar, CERN 1996.

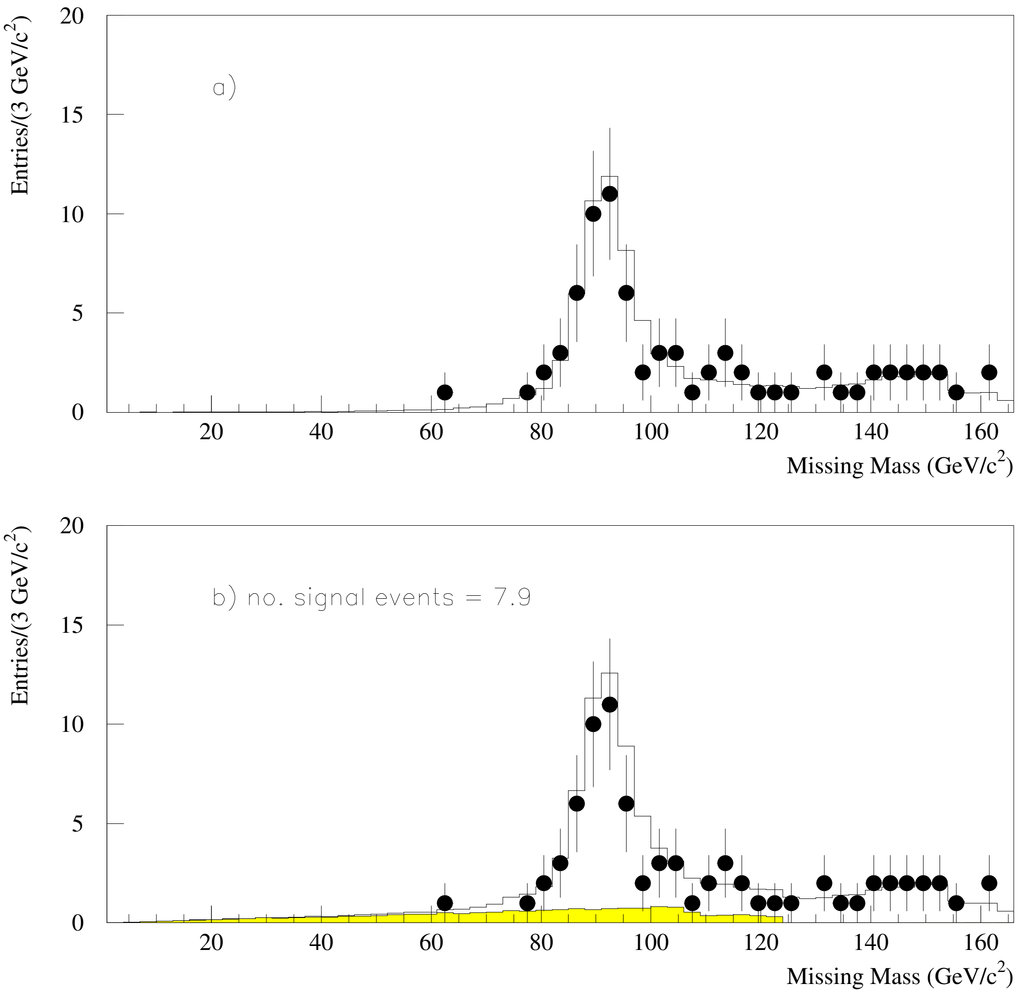

Figure 2: a) The invariant mass distribution of the system recoiling against the photon candidate is shown for both the data (points with error bars) and Monte Carlo (histogram). b) The invariant mass distribution of the system recoiling against the photon candidate is shown for both the data (points with error bars) and Monte Carlo (histogram) plus signal (hatched histogram). A neutralino mass of 120 GeV is plotted for the signal. The area of the signal distribution is 7.9 and the confidence level between data and Monte Carlo plus signal is only 5%. Thus the upper limit on the number of signal events for a 120 GeV mass neutralino is 7.9 at 95% C.L.

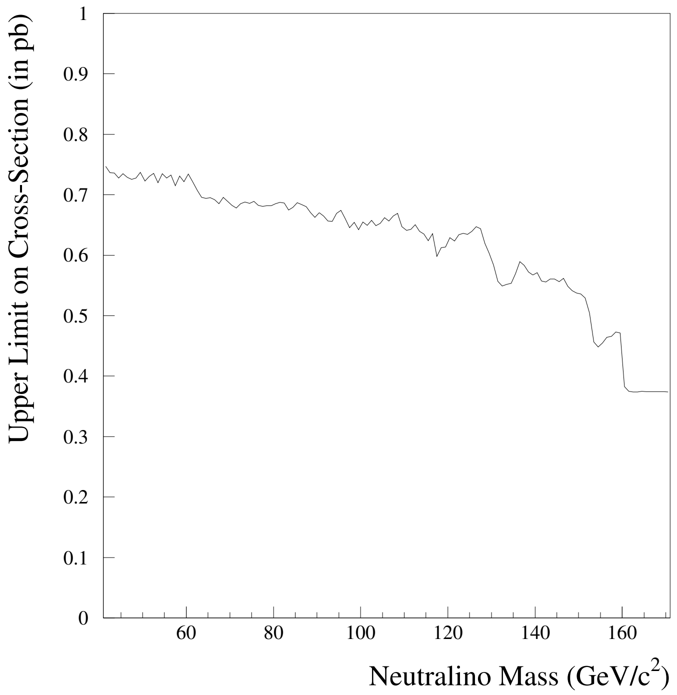

Figure 3: The 95% C.L. upper limit on the production cross-section for $e^+e^- \to \chi_1\tilde{G} \to \tilde{G}\tilde{G}\gamma$. The limit is valid for $\sqrt{s} = 172$ GeV assuming β^8 threshold dependence and isotropic decays.

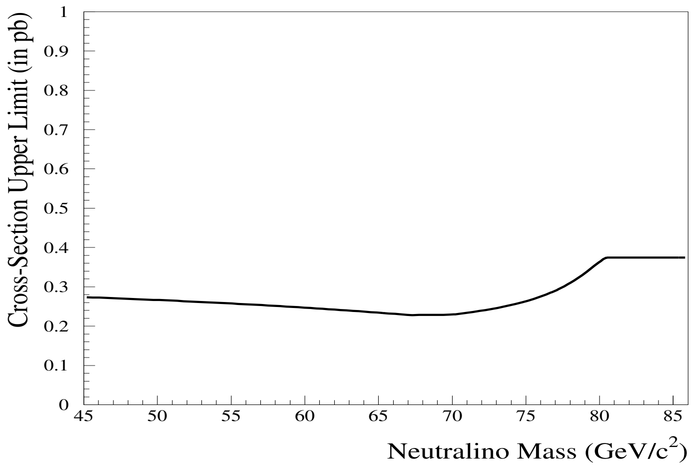

Figure 4: The 95% C.L. upper limit on the production cross section for $e^+e^- \to \chi_1\chi_1 \to \tilde{G}\tilde{G}\gamma\gamma$ when χ_1 has a lifetime less than 3 ns. The limit is valid for $\sqrt{s} = 172$ GeV assuming β^3 threshold behavior and isotropic decays.

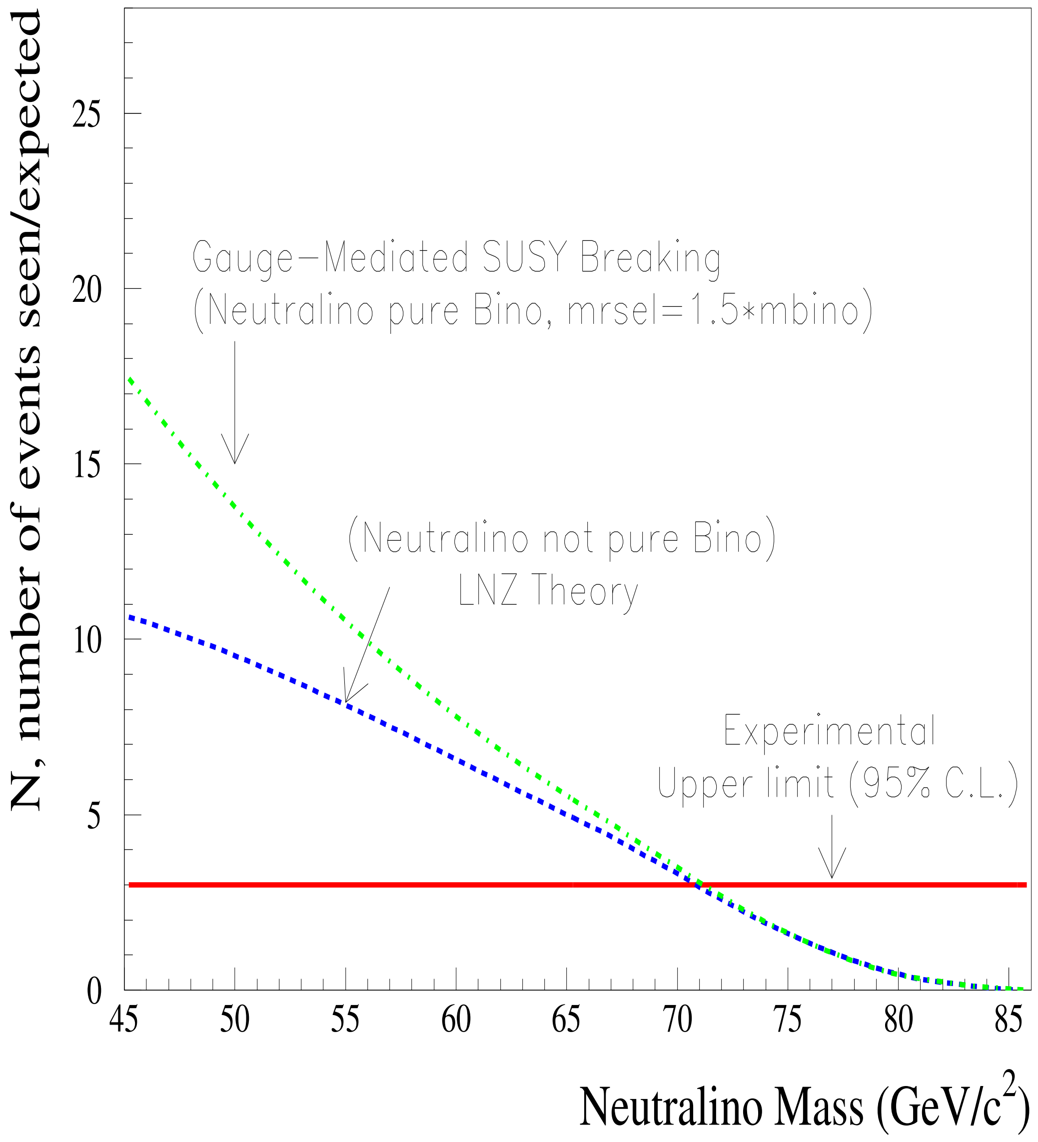

Figure 5: The 95% C.L. exclusion limit for the χ_1 compared to two different $\tilde{G}$ LSP theories. Note that the cross section is not sensitive to the mass of the left-handed selectron.

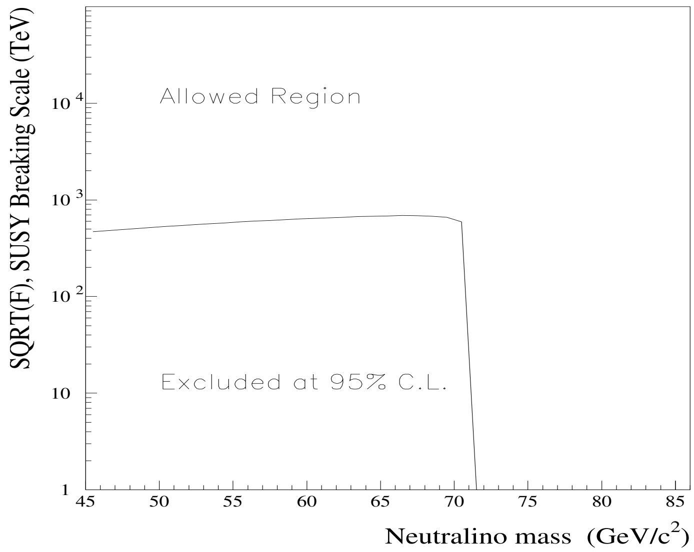

Figure 6: The excluded region in the neutralino mass, $\sqrt{F}$ plane, where the selectron mass is set to 1.5 times the neutralino mass and the neutralino composition is pure bino. There is a cosmological upper bound on $\sqrt{F}$ at 10^5 TeV from nuclear synthesis [23].

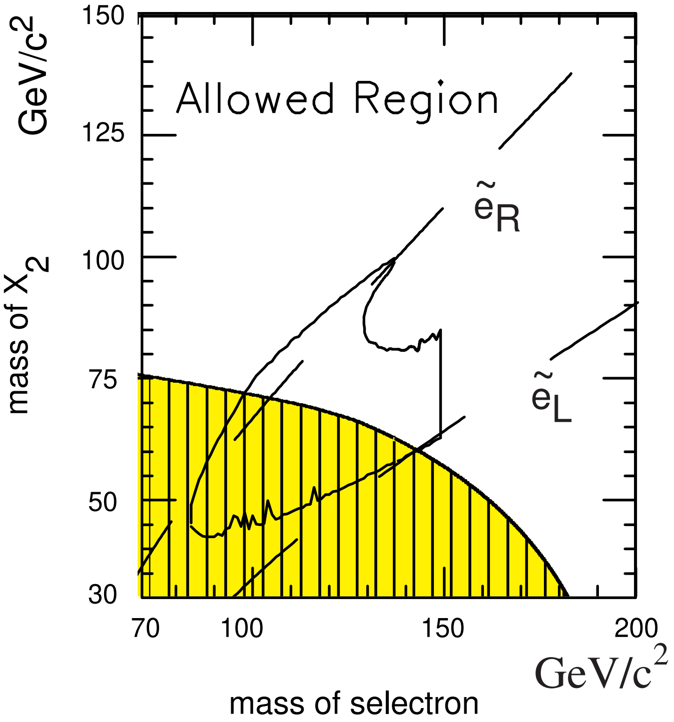

Figure 7: The indicated CDF region determined from the properties of the CDF event assuming the reaction $q\bar{q} \to \tilde{e}\tilde{e} \to ee\chi_1\chi_1 \to ee\tilde{G}\tilde{G}\gamma\gamma$ (taken from the LNZ paper [6]); the region has been cutoff (vertical line) where the prediction rate becomes uninterestingly small. Also delineated are the theoretical masses from the LNZ theory for the right-handed selectron and left-handed selectron (dashed lines). Overlayed is the excluded mass region at 95% C.L. for a pure bino neutralino (hatched area).

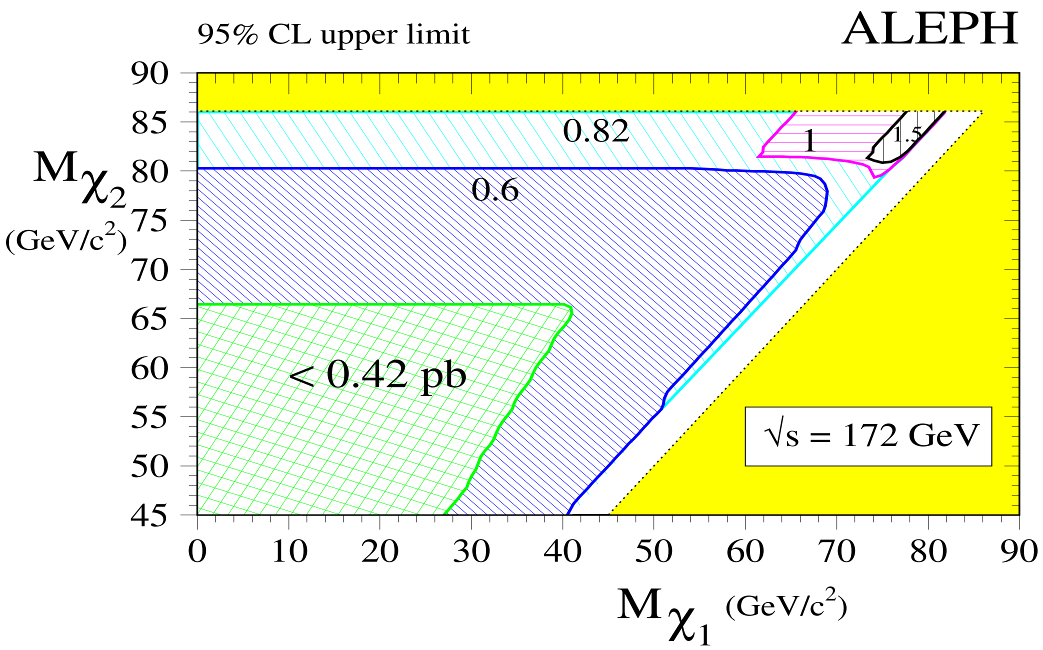

Figure 8: The 95% C.L. upper limit on the production cross section for $e^+e^- \to \chi_2\chi_2 \to \chi_1\chi_1\gamma\gamma$ multiplied by the BR$(\chi_2 \to \chi_1\gamma)$ squared. The limit is valid for $\sqrt{s}$ = 172 GeV assuming β threshold behavior and isotropic decays.

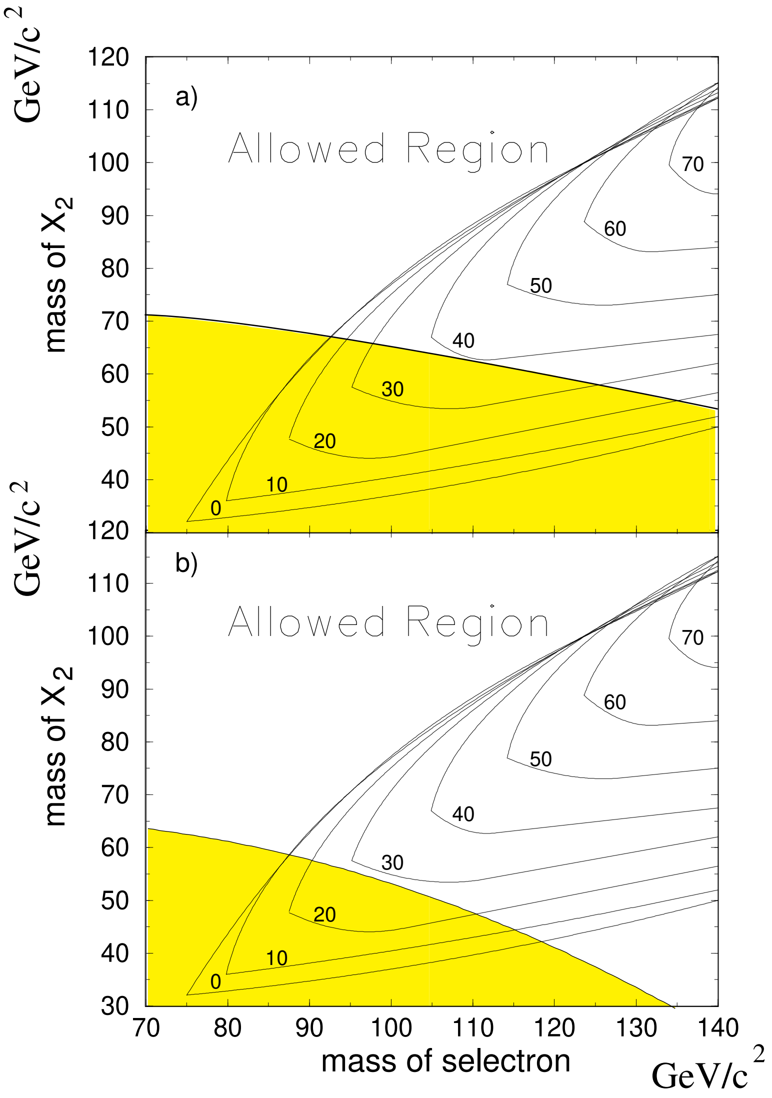

Figure 9: a) The CDF region labeled by the mass of χ_1 in GeV/c^2. This is the area determined from the properties of the CDF event assuming the reaction $q\bar{q} \rightarrow \tilde{e}\tilde{e} \rightarrow ee\chi_2\chi_2 \rightarrow ee\chi_1\chi_1\gamma\gamma$ (taken from [5]). The hatched area is the experimental exclusion region at 95% C.L. for the choice of parameters $M_{\tilde{e}_L} = M_{\tilde{e}_R}$, $\tan\beta = 1.0$, $M_1 = M_2$ and $\mid \mu \mid < 0$. The excluded region is based on the assumptions that χ_2 is pure photino and χ_1 is pure higgsino. The mass limit is independent of the higgsino mass as long as $\Delta M \geq 20$ GeV/c^2. b) Same as a), but here $M_{\tilde{e}_L} = 3{*}M_{\tilde{e}_R}$. The x-axis is the right-handed selectron mass.